ISSN: 0973-3469, Vol.22, No.(2) 2025, Pg. 158-166

Material Science Research India

www.materialsciencejournal.org

Theoretical Insights into Hydrogen Bonding, IR Spectra, and Reactivity of Pimelic Acid in Mixed Solvents using DFT Calculations

SANDIP B. NAHIRE

Department of Chemistry, Mahatma Gandhi Vidyamandir's M.S.G. Arts, Science and Commerce College, SP Pune University, Pune, India.

Abstract

This study explores the structural, vibrational, and electronic behavior of pimelic acid (PA) in different solvent environments—pure, binary (PA–water and PA–ethanol), and ternary (PA–water–ethanol)—using density functional theory (DFT) at the B3LYP/6-311+G(d,p) level. Geometry optimization, vibrational frequency analysis, and molecular orbital calculations were performed to examine hydrogen bonding interactions, IR spectral shifts, and global reactivity descriptors. Results show that the –OH bond distance and stretching frequencies are significantly affected by solvation. Stronger hydrogen bonding was observed in the PA–ethanol complex than in PA–water, with the ternary PA–water–ethanol system (PAWE) exhibiting cooperative effects from both solvents. Intermolecular H-bond distances and frequency shifts confirmed the presence and strength of solute–solvent interactions. Frontier molecular orbital (FMO) analysis revealed solvent-induced variations in the HOMO–LUMO gap, indicating changes in reactivity and stability. Global descriptors—electronegativity, chemical hardness, softness, and electrophilicity—further support the influence of solvent polarity on the reactivity profile of PA. These findings provide theoretical insight into solvation effects on PA, contributing to a better understanding of their chemical behavior in mixed solvent systems.

Article History
Received: 18 July 2025
Accepted: 09 September 2025

Keywords
Density Functional Theory;
Global Reactivity Descriptors;
Hydrogen Bonding;
HOMO–LUMO Gap;
Pimelic Acid;
Solvent Effects.

Introduction

Pimelic acid [1,7-heptanedioic acid, $(CH_2)_5(COOH)_2$; molar mass: 160.17 g mol^{-1}; CAS No. 111-16-0] is a linear aliphatic dicarboxylic acid that serves as a versatile intermediate in the chemical and pharmaceutical industries. It is widely used in the synthesis of pharmaceuticals, surfactants, flavors, and cosmetic ingredients, primarily due to its role

CONTACT Sandip B. Nahire nahiresandip@gmail.com Mahatma Gandhi Vidyamandir's M.S.G. Arts, Science and Commerce College, Malegaon, Nashik, India.

Doi: http://dx.doi.org/10.13005/msri/220206

as a precursor for 1,7-heptanediol. Additionally, pimelic acid has been employed in biochemical studies and as a key building block in organic synthesis pathways.[1-3] Understanding the molecular interactions of such acids in solvent systems is critical for applications involving solubility, reactivity, and formulation development. In this context, Density Functional Theory (DFT) has emerged as a powerful computational technique for probing the structural, electronic, and vibrational characteristics of organic molecules in various environments. Numerous studies have demonstrated the efficacy of DFT—particularly using the B3LYP functional with the 6-311+G(d,p) basis set—in elucidating solute–solvent interactions, hydrogen bonding, vibrational frequency shifts, and global reactivity descriptors.[4-5] For instance, in our previous study,[6] we conducted a comprehensive DFT and experimental investigation on glutaric acid in water–ethanol binary mixtures, where we evaluated solubility, intermolecular hydrogen bonding, vibrational spectra, and global chemical reactivity indices. The study demonstrated that solvation significantly influences the O–H stretching frequencies and hydrogen bond distances, with findings supported by correlated thermodynamic data. This methodology was further extended in our subsequent work[7] on malonic acid in aqueous alcohol mixtures, where we combined solubility measurements with DFT calculations to derive insights into HOMO–LUMO energies, IR spectral behavior, and thermodynamic functions. These studies collectively highlight the critical role of solvent polarity and hydrogen bonding capacity in modulating the structural and electronic properties of dicarboxylic acids. Complementing these efforts, Hammami and Issaoui explored hydrogen-bonded clusters of pyruvic acid with water using DFT, revealing how micro solvation modulates IR signatures and stabilizes specific conformers through strong hydrogen bonding.[8] Furthermore, Pushparaju *et al.*[9] applied B3LYP/6-311G(d,p) to study alkoxybenzoic acid-based hydrogen-bonded systems, calculating HOMO–LUMO energy gaps, polarizability, and IR frequencies to characterize their liquid crystalline behavior. Updated DFT and IR analyses of tartaric acid confirmed strong hydrogen-bonding contributions to vibrational band shifts, further validating DFT approaches in carboxylic acids.[10] Intermolecular hydrogen bonding in ternary liquid crystalline mixtures was recently examined by FTIR spectroscopy, highlighting cooperative hydrogen-bonding effects comparable to our PA–water–ethanol system.[11] Similar insights were reported for azelaic acid complexes in coordination chemistry, where DFT revealed hydrogen bonding as a key stabilizing factor.[12]

These studies establish a strong methodological foundation for applying DFT to PA in mixed solvent systems. However, a detailed theoretical investigation of PA in water–ethanol mixtures—focusing on hydrogen bonding dynamics, vibrational shifts, reactivity indices, and IR spectral features—remains underexplored. The present study aims to address this gap by employing DFT calculations at the B3LYP/6-311+G(d,p) level to investigate the structural and electronic modifications in pimelic acid resulting from interactions with binary and ternary solvent systems. Although Gaussian 03 is not the most recent version, it was used in the present study to ensure consistency and reproducibility with our earlier related works.[6-7]

Computational Methodology

A comprehensive computational study was conducted to elucidate the molecular interactions influencing the solution behavior of PA. Geometry optimizations of the isolated molecule, as well as its binary and ternary solvent complexes, were performed using the Gaussian 03 software package.[13] All density functional theory (DFT) calculations were carried out on a Windows 10 platform equipped with an Intel Core i7 processor and 16 GB of RAM. The B3LYP functional in combination with the 6-311+G(d,p) basis set was employed to obtain optimized geometries and electronic properties. Vibrational frequencies were computed at the B3LYP/6-311+G(d,p) level and scaled by a factor of 0.9679, consistent with standard literature practice for this basis set. Dispersion corrections (Grimme's D3) were not included, as the primary focus was on hydrogen-bonding-driven interactions, where B3LYP/6-311+G(d,p) has been shown to give reliable geometries and vibrational trends in previous studies.[4-9] The computational analysis was designed to elucidate solvent–solvent and solute–solvent interactions at the molecular level. DFT-based FTIR spectral analysis revealed characteristic shifts in the –OH stretching frequencies, indicative of hydrogen bond formation within binary solvent mixtures and

ternary solute–solvent systems. These frequency shifts provide insights into the nature and strength of the intermolecular interactions involved.[14]

The dipole moment of a molecule, defined as the product of charge separation and the distance between charges, is directly related to molecular polarizability and solubility. Molecules with large ground-state dipole moments exhibit stronger interactions with polar solvents owing to the solvent polarity effects.[15-18] Furthermore, molecular polarizability and atomic electron density distribution are correlated with frontier molecular orbitals, that is, the highest occupied molecular orbital (HOMO) and lowest unoccupied molecular orbital (LUMO), which influence the chemical reactivity and solubility.[19-21] A recent combined DFT–thermodynamic study on carboxyl-based solvents further emphasized how hydrogen bonding and solvent polarity regulate solute stability and reactivity.[22]

A key parameter derived from DFT is the HOMO–LUMO energy gap, which provides insight into chemical reactivity and electronic stability:

HOMO - LUMO Energy Gap = Energy of LUMO – Energy of HOMO ...(1)

All orbital energies were expressed in electron volts (eV). If the energy gap is computed in Hartrees (atomic units), it is converted to eV using

Energy gap (eV) = Energy gap (Hartree or a.u.) × 27.21138602 ...(2)

In this work, only explicit solvent clusters (PAW, PAE, and PAWE) were considered, as our aim was to directly probe solute–solvent hydrogen-bonding interactions. No implicit solvation model (PCM/SMD) was applied in combination, in order to isolate and characterize the effects of explicit hydrogen bonds. The PA–water–ethanol (PAWE) complexes were built from binary-optimized minima (PAW and PAE) and fully re-optimized without symmetry constraints to confirm true minima (no imaginary frequencies).

Electrochemical Properties

Frontier molecular orbital (FMO) energies provide insight into the electronic stability and reactivity of molecules. The HOMO energy (E_{HOMO}) reflects the electron-donating ability, while the LUMO energy (E_{LUMO}) indicates electron-accepting potential; their separation defines the HOMO–LUMO gap, a key descriptor of chemical reactivity.[23-24]

Global reactivity descriptors such as electronegativity (χ), chemical potential (μ), chemical hardness (η), softness (σ), electrophilicity index (ω), ionization potential (I), and electron affinity (A) were obtained from E_{HOMO} and E_{LUMO} using Koopmans' theorem-based formulations[25] and standard treatments described in the literature.[26] These indices offer quantitative measures of the stability and reactivity profile of pimelic acid in different solvent environments.

Results and Discussion

The optimized geometries of PA and its solvent-associated complexes are illustrated in Fig. 1. The corresponding structural and electronic properties derived from these optimizations are summarized in Tables 1 and 2. It is observed that the zero-point vibrational energy (ZPVE) and nuclear repulsion energy of PA increase upon complexation with both single and binary solvent molecules. Similarly, the absolute total energy, isotropic polarizability, and theoretically computed thermodynamic parameters of PA also exhibit an increasing trend in the presence of solvent interactions. As shown in Table 1, the –O–H bond length of the carboxylic group in isolated PA is greater than that in the PAW and PAE complexes. Among the pure solvent combinations, the bond length follows the order: PAE > PAW. Furthermore, the carboxylic –O–H bond distance in the ternary PA-water-ethanol (PAWE) complex is found to be longer than that in isolated PA, indicating enhanced solute–solvent interactions in the mixed solvent environment.

Table 1 also presents the intermolecular hydrogen bond (H-bond) distances between pimelic acid (PA) and its solvent complexes. The H-bond distances—specifically between a hydrogen atom of the carboxylic group in PA and an oxygen atom of the solvent (-H···O-), as well as between an oxygen atom of the carboxylic group and a hydrogen atom from the solvent (-O···H-)—follow the trend: PAE < PAW. This suggests stronger hydrogen bonding interactions in the PA–ethanol complex compared to the PA–water complex. A similar trend is observed in the ternary PAWE complex, further supporting this conclusion. As the optimized

hydrogen bond distances (Table 1) clearly show consistent shortening in the ethanol complexes relative to water, additional statistical analysis or binding energy decomposition was not pursued, since such treatments fall beyond the scope of the present structural–vibrational focus

Table 1: Calculated υ-OH (–OH str.freq.), -OH bond distance, intermolecular H-bond distance for pure substance, binary solvents and ternary solution by DFT/ B3LYP method at 6-311G +(d p) basis set

System	Carboxylic υ-OH cm^{-1}	Carboxylic (-OH) Bond Dist. (Å)	Inter Molecular H-Bond Dist. (Å) O-H	Inter Molecular H-Bond Dist. (Å) C=O-H	Zero point vibration energy Kcal/mol	Nuclear Repulsion Energy Hartrees
PA	3758.6	0.9691	-	-	119.558	582.982
W	3818.57	0.9619	-	-	13.3592	9.1571
E	3843.85	0.9617	-	-	49.9302	81.6031
WE	3838.35	0.9626	1.9011	-	65.2986	131.056
PAW	3419.28	0.9863	1.8058	2.0414	135.306	679.349
PAE	3330.73	0.9907	1.7611	2.0173	171.048	850.539
PAWE	3420.97	0.9862	1.8074	1.987	186.78	956.713
	3338.82	0.9905	1.7636	2.0292		

Table 2: Theoretical Computed total energy, isotropic polarizability (α), thermodynamic function calculated by DFT/B3LYP method and 6-311G (+d p) basis set. [PA, solvents and its combinations]

System	E (RB3LY) a.u.	(α) $Bohr^3$	Total Energy (a.u.)		
			E (Thermal) Kcal/mo	C_v cal/mol/K	S Cal/mol.K
PA	-575.0946	97.079	127.401	43.060	115.670
W	-76.4584	7.29	45.087	15.139	6.014
E	-115.095	30.90	64.711	52.658	13.615
WE	-231.563	39.49	23.735	70.142	85.735
PAW	-651.569	106.27	144.923	52.240	131.005
PAE	-730.206	130.72	182.357	60.564	149.333
PAWE	-806.681	139.95	199.858	69.755	162.860

The results of the theoretical vibrational frequency analysis for PA and its solvent complexes are presented in Table 1 and illustrated graphically in Fig. 3. The –OH stretching frequency of carboxylic acid in pure PA is higher compared to that in PAW and PAE complexes. Among the binary solvent systems, the observed order of increasing –OH stretching frequency is: PAE (3330.73 cm^{-1}) < PAW (3419.28 cm^{-1}), indicating a more pronounced red shift in ethanol. Experimental IR studies of related dicarboxylic acids in hydrogen-bonded environments typically report –OH stretching bands in the range of 3300–3500 cm^{-1}.[27, 28] The computed values (after applying the 0.9679 scaling factor) fall within this range, confirming that the observed red shifts are consistent with literature expectations. This significant difference suggests that stronger solute–solvent interactions occur in the PAE complex than in the PAW system. Furthermore, the –OH stretching frequency in the ternary complex (PAWE) is lower than that of pure PA, implying the presence of additional intermolecular hydrogen bonding in the PAWE system.

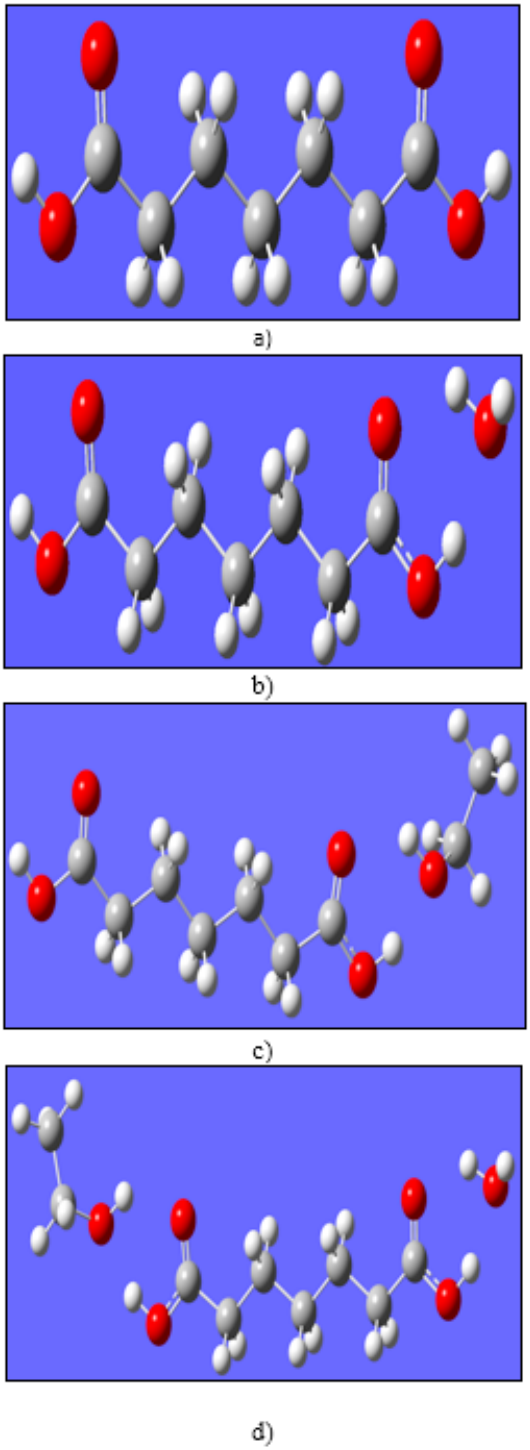

Fig 1: Optimized geometries of PA and solvent complexes obtained at the B3LYP/6-311+G(d,p) level a) PA b) PAW c) PAE d) PAWE

Table 3: HOMO-LUMO energies and energy gap between LUMO-HOMO

System	HOMO ev	LUMO ev	LUMO-HOMO energy gap (eV)
PA	-7.9879	-0.2811	7.7068
W	-8.7896	-0.5203	8.2693
E	-7.6342	-0.0457	7.5884
WE	-7.9569	-0.2746	7.6823
PAW	-7.9795	-0.2650	7.7144
PAE	-7.7909	-0.2449	7.5460
PAWE	-7.7855	-0.2191	7.5664

The HOMO and LUMO energies, along with the corresponding HOMO–LUMO energy gap, are presented in Table 3 and illustrated graphically in Fig. 2. Relative to isolated PA (7.71 eV), the HOMO–LUMO gap changes by +7.3% in water, –1.5% in ethanol, and ~ –2% in ternary systems. These quantitative variations support the claim that solvent polarity and hydrogen bonding modulate the electronic stability and reactivity of PA. The values of HOMO–LUMO energy gap were further utilized to compute the global chemical reactivity indices, summarized in Table 4. The electrophilicity index (ω) is higher in ethanol-containing systems (PAE: 2.14 eV; PAWE: 2.12 eV) than in water (PAW: 2.20 eV), indicating greater electron-accepting ability and enhanced susceptibility of PA toward nucleophilic attack at the carboxyl carbon. This agrees with earlier findings that solvation enhances the electrophilic power of neutral molecules, thereby favoring esterification reactivity in ethanol-rich media while water stabilizes PA through stronger hydration.[29] Parallel DFT studies on adipic acid have revealed solvent-dependent hydrogen bonding as a determinant of reactivity in catalytic environments.[30] Recent mechanistic studies on aliphatic carboxylic acids also demonstrated that solvent polarity and hydrogen bonding tune reactivity patterns, supporting the trends observed in this work.[31]

Fig. 2: HOMO, LUMO structures with LUMO-HOMO energy gap

Molecule	HOMO	Energy Gap	LUMO
PA	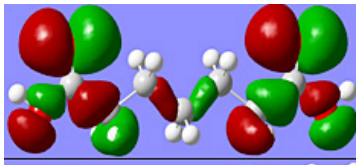	7.7068	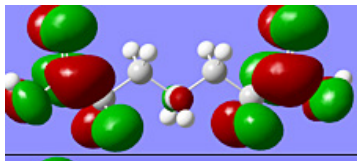
PAW	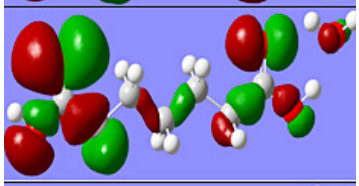	8.2693	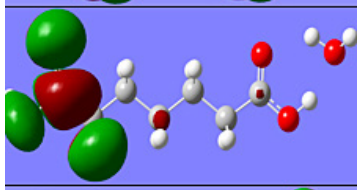
PAE	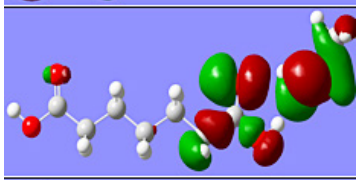	7.5884	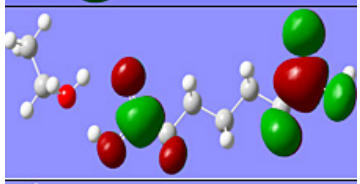
PAWE	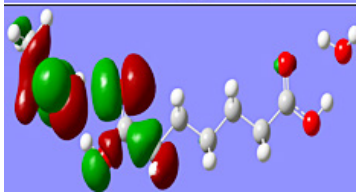	7.6823	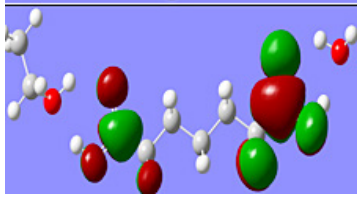

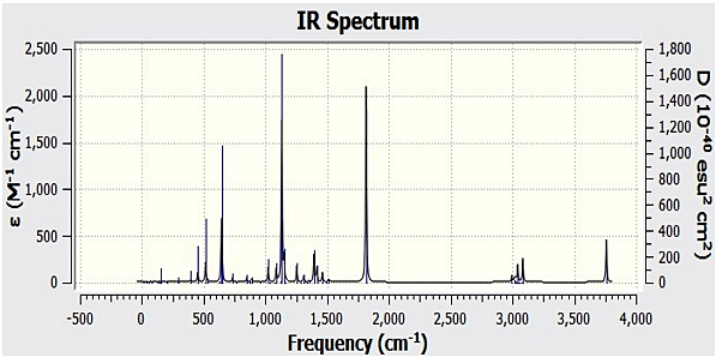

1. Theoretical IR of PA

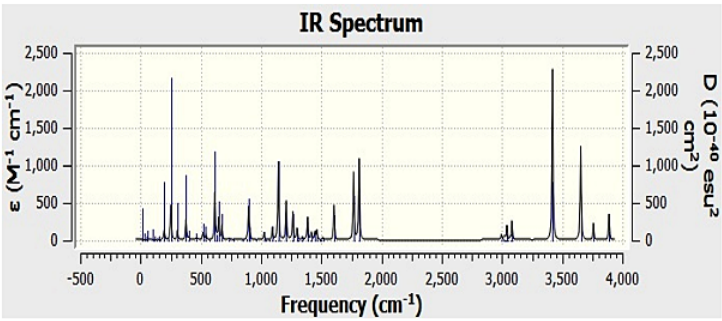

2. Theoretical IR of PAW

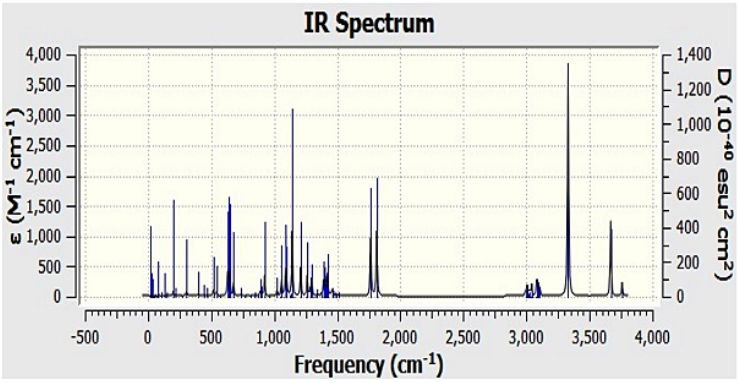

4. Theoretical IR of PAE

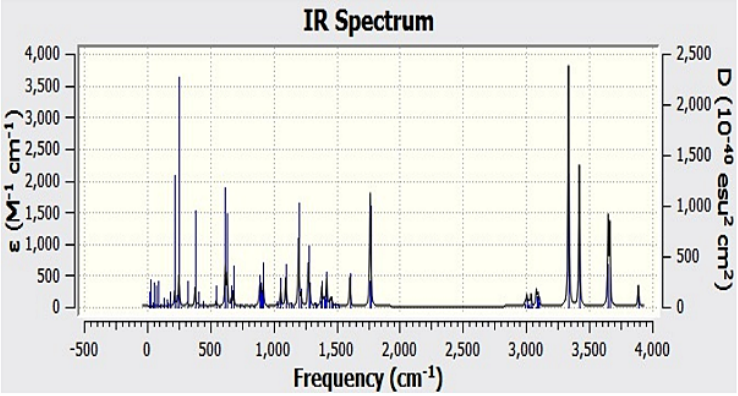

7. Theoretical IR of PAWE

Fig. 3:Theoretical I.R. spectra in gas phase by DFT/B3LYP at 6-311G (+d p) basis set

Table 4: Global chemical reactivity indices

system	η eV	σ eV	χ eV	μ eV	ω eV	A eV	I eV
PA	3.8534	0.2595	4.1345	-4.1345	2.2180	7.9879	0.2811
W	4.1346	0.2419	4.6549	-4.6549	2.6203	8.7896	0.5203
E	3.7942	0.2636	3.8399	-3.8399	1.9431	7.6342	0.0457
WE	3.8412	0.2603	4.1157	-4.1157	2.2050	7.9569	0.2746
PAW	3.8572	0.2593	4.1223	-4.1223	2.2028	7.9795	0.2650
PAE	3.7730	0.2650	4.0179	-4.0179	2.1393	7.7909	0.2449
PAWE	3.7832	0.2643	4.0023	-4.0023	2.1170	7.7855	0.2191

Conclusion

The DFT analysis of pimelic acid (PA) in pure, binary, and ternary solvent environments demonstrates that solvation significantly modulates its structural, vibrational, and electronic properties. Quantitatively, the HOMO–LUMO gap decreased by 0.16 eV in ethanol (PAE: 7.55 eV) compared to isolated PA (7.71 eV), while water increased the gap by ~7% (8.27 eV). Similarly, hydrogen bond distances were shorter in ethanol (1.76 Å) than in water (1.81 Å), confirming stronger solute–solvent interactions in ethanol-rich media.

These solvent-induced changes are not only of theoretical interest but also carry broader chemical relevance. Modulation of the electrophilicity index (ω) by solvent polarity indicates that ethanol promotes stronger hydrogen bonding and facilitates

accessibility of the carboxyl carbon to nucleophiles, consistent with PA's role in esterification and related reactions. Such insights are useful for industrial formulation and solvent selection, where mixed solvents like water–ethanol can provide a tunable balance between reactivity and stability. From a green chemistry perspective, water–ethanol mixtures represent sustainable media that optimize reactivity while minimizing reliance on harsher solvents.

Acknowledgement
The author is thankful to Principal of MSG Arts, Science and Commerce College Malegaon for providing DFT software. The authors also express their sincere thanks to Dr Apoorva Hiray (Co-ordinator M.G. Vidyamandir Malegaon).

Funding Sources
The author(s) received no financial support for the research, authorship, and/or publication of this article.

Conflict of Interest
The authors do not have any conflict of interest.

Data Availability Statement
This statement does not apply to this article.

Ethics Statement
This research did not involve human participants, animal subjects, or any material that requires ethical approval.

Clinical Trial Registration
This research does not involve any clinical trials.

Permission to Reproduce Material from Other Sources
Not Applicable.

Author Contributions
The sole author was responsible for the conceptualization, methodology, data collection, analysis, writing, and final approval of the manuscript.

References

1. J.C. Espinosa-Lara, D. Guzman-Villanueva, J.I. Arenas-García, D. Herrera-Ruiz, J. Rivera-Islas, P. Román-Bravo, H. Morales-Rojas, H. Höpfl, Cocrystals of active pharmaceutical ingredients Praziquantel in combination with oxalic, malonic, succinic, maleic, fumaric, glutaric, adipic, and pimelic acids. *Cryst. Growth Des.* 13, 169–185 (2013).
2. J. Cason, L. Wallcave, C.N. Whiteside, A convenient preparation of suberic acid. Concerning the homogeneity and use in synthesis of polymethylene chlorobromide preparations. *J. Org. Chem.* 14, 37–44 (1949).
3. H. Li, X. Jiao, X. Chen, Thermodynamic analysis for solubility of pimelic acid in ionic liquids. *Russ. J. Phys. Chem.* A 88, 1133-1137 (2014).
4. G. Buemi, DFT study of the hydrogen bond strength and IR spectra of formic, oxalic, glyoxylic and pyruvic acids in vacuum, acetone and water solution. *J. Phys. Org. Chem.* 22, 933–947 (2009).
5. Z. Dou, L. Wang, J. Hu, W. Fang, C. Sun, Z. Men, Hydrogen bonding effect on Raman modes of formic acid–water binary solutions. *J. Mol. Liq.* 313, 113595 (2020).
6. R.R. Pawar, S.B. Nahire, Measurement, correlation and DFT study for solubility of glutaric acid in water + ethanol binary solvents at T = (293.15 to 313.15) K. *Asian J. Res. Chem.* 13, 169–174 (2020).
7. R.R. Pawar, S.B. Nahire, Investigation, correlation and DFT study for solubility of malonic acid in water–methanol and water–ethanol binary solvents at T = 293.15 to 313.15 *K. Res. J. Pharm. Technol*. 14, 1226–1232 (2021).
8. F. Hammami, N. Issaoui, A DFT study of the hydrogen bonded structures of pyruvic acid–water complexes. *Front. Phys.* 10, 901736 (2022).
9. P. Subhapriya, K. Sadasivam, M.M. Mohan, P.S. Vijayanand, Experimental and theoretical investigation of p–n alkoxy benzoic acid based liquid crystals–A DFT approach. *Spectrochim. Acta A Mol. Biomol. Spectrosc.* 123, 511–523 (2014).
10. C. Tsioptsias, S. Matsia, A. Salifoglou, Revisiting the Thermal Behavior and Infrared Absorbance

Bands of Anhydrous and Hydrated DL-Tartaric Acid, *Int. J. Mol. Sci.* 26, 12029899 (2025).
11. M. Rakshan, M.S. Ismail, S. Manoj, T.A. Krithic, Mechanistic insights into dielectric relaxations of ternary liquid crystalline mixtures formed via intermolecular hydrogen bonding, *J. Mol. Liq.* 423, 132042 (2025).
12. M. Benito, G. Mahmoudi, E. Molins, E. Zangrando, Versatile copper (II) discrete and polymeric coordination compounds with (pyridine-2-yl) methylenenicotinohydrazide and azelaic acid, *CrystEngComm* 27, 1021 (2025).
13. M.J. Frisch, G.W. Trucks, H.B. Schlegel, G.E. Scuseria, M.A. Robb, J.R. Cheeseman, J.J.A. Montgomery, T. Vreven, K.N. Kudin, J.C. Burant, Gaussian 03, Revision C.02, Gaussian Inc., Wallingford CT (2004).
14. M.S. Raman, M. Kesavan, K. Senthilkumar, V. Ponnuswamy, Ultrasonic, DFT and FT-IR studies on hydrogen bonding interactions in aqueous solutions of diethylene glycol. *J. Mol. Liq*. 202, 115–124 (2015).
15. K. Hatua, P.K. Nandi, Relationships between different-order polarizabilities and ground state dipole moment. *J. Theor. Comput. Chem*. 12, 1250099 (2013).
16. T.Y. Lin, A. Chaudhari, S.L. Lee, Correlation between substituent constants and hyperpolarizabilities for di-substituted trans-azobenzenes. *J. Mol. Model.* 19, 529–538 (2013).
17. S.A. Blair, A.J. Thakkar, Relating polarizability to volume, ionization energy, electronegativity, hardness, moments of momentum, and other molecular properties. *J. Chem. Phys.* 141, 074306 (2014).
18. A. Masternak, G. Wenska, J. Milecki, B. Skalski, S. Franzen, Solvatochromism of a novel betaine dye derived from purine. *J. Phys. Chem.* A 109, 759–766 (2005).
19. R.S. Dumont, Effects of charging and polarization on molecular conduction via the source-sink potential method. *Can. J. Chem.* 92, 100–111 (2014).
20. I.H. Jung, W.Y. Lo, J. Jang, W. Chen, D. Zhao, E.S. Landry, L. Lu, D.V. Talapin, L. Yu, Synthesis and search for design principles of new electron accepting polymers for all-polymer solar cells. *Chem. Mater.* 26, 3450–3459 (2014).
21. S.H. Gallagher, R.S. Armstrong, P.A. Lay, C.A. Reed, Solvent effects on the electronic spectrum of C60. *J. Phys. Chem.* 99, 5817–5825 (1995).
22. J. Wang, C. Ma, X. Ge, Z. Zhong, Q. Zhang, Thermodynamic Properties and Internal Interaction Behavior of Carboxyl-Based Deep Eutectic Solvents with 1,4-Butylactone Binary Mixtures by a Combined DFT Approach, *J. Chem. Eng*. Data 70, 698 (2025).
23. F.Y. Li, J.J. Zhao, Quantum chemistry PM3 calculations of sixteen mEGF molecules. *J. At.* Mol. Sci. 1, 68–77 (2010).
24. E. Mohammad, A. Kanaani, The effect of solvent polarity on solubility of HMX and FOX7: A DFT study. *Indian J. Pure Appl. Phys*. 55, 490–496 (2017).
25. T. Koopmans, On the assignment of wave functions and eigenvalues to the individual electrons of an atom. *Physica* 1, 104–113 (1934).
26. R. G. Parr, W. Yang, Density-Functional Theory of Atoms and Molecules. Oxford University Press, New York (1989).
27. M. H. Brooker, Spectroscopic studies of aqueous carboxylic acids. *Can. J. Chem.* 52, 3661–3667 (1974).
28. G. Socrates, Infrared and Raman Characteristic Group Frequencies, Wiley, 2001.
29. L.R. Domingo, J.A. Sáez, P.M. Peiró, E. Chamorro. Solvent effect on the electrophilicity index. *J. Org. Chem.* 67 (26), 8917–8922 (2002).
30. D.K. Mishra, C.C. Truong, Y. Jo, Recent catalytic advances in the production of adipic acid and its esters from bio-based C6 molecules and carbon dioxide, *Green Chem. Eng.* 2, 2457497 (2025).
31. J. Liu, L. Huang, Z. Sun, J. Li, γ-1,1-C(sp3)–H activation of aliphatic carboxylic acids: mechanistic pathways, substituent influence on product selectivity, diastereoselectivity, and additive effects, *Org. Chem. Front.* 11, 1451 (2024).